Published in final edited form as:
Development. 2008 February ; 135(4): 659–667. doi:10.1242/dev.013623.

The netrin receptor UNC5B promotes angiogenesis in specific vascular beds

Sutip Navankasattusas[1,*], **Kevin J. Whitehead**[1,2,*], **Arminda Suli**[3], **Lise K. Sorensen**[1], **Amy H. Lim**[3], **Jia Zhao**[1], **Kye Won Park**[1,†], **Joshua D. Wythe**[1,4], **Kirk R. Thomas**[1,5], **Chi-Bin Chien**[3,6,‡], and **Dean Y. Li**[1,2,4,‡]

1 *Program in Human Molecular Biology and Genetics, University of Utah, Salt Lake City, UT 84112, USA*

2 *Division of Cardiology, Department of Internal Medicine, University of Utah, Salt Lake City, UT 84112, USA*

3 *Department of Neurobiology and Anatomy, University of Utah, Salt Lake City, UT 84112, USA*

4 *Department of Oncological Sciences, University of Utah, Salt Lake City, UT 84112, USA*

5 *Division of Hematology, Department of Internal Medicine, University of Utah, Salt Lake City, UT 84112, USA*

6 *Brain Institute, University of Utah, Salt Lake City, UT 84112, USA*

Abstract

There is emerging evidence that the canonical neural guidance factor netrin can also direct the growth of blood vessels. We deleted the gene encoding UNC5B, a receptor for the netrin family of guidance molecules, specifically within the embryonic endothelium of mice. The result is a profound structural and functional deficiency in the arterioles of the placental labyrinth, which leads first to flow reversal in the umbilical artery and ultimately to embryonic death. As this is the only detectable site of vascular abnormality in the mutant embryos, and because the phenotype cannot be rescued by a wild-type trophectoderm, we propose that UNC5B-mediated signaling is a specific and autonomous component of fetal-placental angiogenesis. Disruption of UNC5B represents a unique example of a mutation that acts solely within the fetal-placental vasculature and one that faithfully recapitulates the structural and physiological characteristics of clinical uteroplacental insufficiency. This pro-angiogenic, but spatially restricted requirement for UNC5B is not unique to murine development, as the knock-down of the *Unc5b* ortholog in zebrafish similarly results in the specific and highly penetrant absence of the parachordal vessel, the precursor to the lymphatic system.

Keywords

Angiogenesis; Netrin; Placenta; UNC5B; Zebrafish; Mouse

‡Authors for correspondence (e-mails: chi-bin.chien@neuro.utah.edu; dean.li@hmbg.utah.edu).
*These authors contributed equally to this work
†Present address: Department of Pathology and Laboratories Medicine, UCLA, Los Angeles, CA 90095, USA

Supplementary material
Supplementary material for this article is available at http://dev.biologists.org/cgi/content/full/135/4/659/DC1

INTRODUCTION

Guidance cues were first identified by their ability to direct axonal projections along specific trajectories. Many of these cues and their cognate receptors have since been shown to play similar roles during angiogenesis, either promoting or directing the growth of growing vessels. A prime example of this is the netrin family, the founding member of which, netrin 1, was originally purified as a secreted guidance cue capable of stimulating growth of commissural axons and attracting them towards the midline (Kennedy et al., 1994; Serafini et al., 1994). Reports from our group and others have shown that netrins can also play a similar role in the vasculature, promoting developmental and therapeutic angiogenesis in a number of in vitro and in vivo systems (Nguyen and Cai, 2006; Park et al., 2004; Wilson et al., 2006).

Netrin signaling is complex, however, and is not always attractive/stimulatory. In mammals there are three netrins and at least eight potential netrin receptors: DCC, neogenin, UNC5A-D, and α6β4 and α3β4 integrins (Cirulli and Yebra, 2007; Huber et al., 2003; Tessier-Lavigne and Goodman, 1996; Yebra et al., 2003). Additional netrin receptors have been postulated, and efforts to identify them are ongoing. Although netrins are the prototypic neural attractants, they can also act as repulsive guidance signals under the appropriate cellular context. One receptor, UNC5B, was identified as a mediator of the repulsive response in neurons (Leonardo et al., 1997), and it is the only known netrin receptor with prominent endothelial expression (Engelkamp, 2002; Lu et al., 2004).

Unc5b is expressed in the endothelium of developing mouse embryos beginning at embryonic day 8.5 (Engelkamp, 2002; Lu et al., 2004). A published study concluded that the axon-repulsive activity mediated by UNC5B is mirrored by an anti-angiogenic role for netrin 1-UNC5B signaling in both mice and zebrafish (Lu et al., 2004). This conclusion was based on observations that the mutation of *Unc5b* resulted in increased sprouting within developing arterial beds, which was interpreted as an indicator of reduced repulsion. This report also postulated that the excessive vascular sprouting caused by the global absence of UNC5B during murine embryogenesis precipitated greater resistance to circulation, resulting in heart failure and fetal demise.

In contrast to the conclusions of Lu and colleagues, our previous analysis of netrin signaling in the vasculature (Park et al., 2004; Wilson et al., 2006) suggested a starkly different situation. We found that the addition of netrins stimulated angiogenesis both in vivo and in vitro, and that the knock-down of *netrin1a* in zebrafish inhibited growth of the parachordal vessel (PAV), a blood vessel that has recently been found essential for lymphatic development (Yaniv et al., 2006).

In an attempt to resolve these different interpretations, we have made use of non-invasive imaging technologies to examine mice carrying a conditional mutant allele of the *Unc5b* gene. Although the vascular-restricted deletion of *Unc5b* indeed causes embryonic lethality, we could find no evidence of either low or high-output heart failure prior to abrupt death at embryonic day 12. Instead, our data showed a previously unappreciated and essential role for UNC5B in promoting placental arteriogenesis. In zebrafish we found a similar pro-angiogenic role, where knocking down *unc5b*, like knocking down *netrin1a*, prevents formation of the PAV.

MATERIALS AND METHODS

Mouse strains

Generation of the *Unc5b* alleles has been described (Wilson et al., 2006). *R26R1*, *Tie2-Cre*, *Vav1-Cre* and *Netrin1:lacZ* mice were generously provided by Phil Soriano, Masashi

Yanagisawa, Matthias Stadtfeld and Lindsay Hinck, respectively. *SM22-Cre* (*Tagln-Cre*), *Nestin-Cre* and *Wnt1-Cre* mice were obtained from The Jackson Laboratory. Genotypes were determined by PCR analysis of genomic DNA isolated from either ear biopsies or yolk sacs; amplification used primers and conditions previously described for *Tie2-Cre* (Kisanuki et al., 2001), *SM22-Cre* (Holtwick et al., 2002), *Nestin-Cre* (Sclafani et al., 2006), *Vav1-Cre* (Stadtfeld and Graf, 2005) and *Rosa26* (Soriano, 1999). For *Wnt1-Cre*, the primers were 5′-AGCAACCACAGTCGTCAGAACC and 5′-AAGATAATCGCGAACATCTTCAGG with amplification of 94°C for 30 seconds, 58°C for 30 seconds, and 72°C for 40 seconds. *Unc5b* mice were genotyped with primers: 5′-TAGCCTCAGGGTCTACTGTCTG; 5′-CTCTCAGACTTCTCAAAGAGATTC; and 5′-CCACTGTATGCCAGACGACATG under conditions of 94°C for 30 seconds, 62°C for 20 seconds and 68°C for 40 seconds.

Histology

Smooth muscle cells were identified by anti-α-smooth muscle actin antibody (Sigma) staining of formaldehyde-fixed, paraffin-embedded tissue sectioned at 10 μm as described previously (Urness et al., 2000). The number of arterioles in the labyrinth was determined by examination of all serial sections from a placental hemisphere. Wild-type and mutant placentas were from paired littermates. β-Galactosidase staining was performed using a standard protocol (Soriano, 1999) with the following modification: the tissues were fixed in PBS containing 2% formaldehyde, 0.2% glutaraldehyde, 0.02% sodium deoxycholate and 0.01% NP-40 for 10–30 minutes. Placentas were hemisected with a razor blade before fixation. The tissues were permeabilized in PBS containing 0.02% sodium deoxycholate and 0.1% NP-40 overnight at 4°C before staining with X-gal.

Staining for PECAM1 was performed on tissues fixed overnight in Dent's fixative (4:1 MEOH: DMSO) at 4°C, followed by bleaching by addition of an equal volume of 37%H_2O_2 for 6–10 hours at room temperature, and storage at −20°C in 100% methanol. Placentas were rehydrated to PBS, hemisected sagittally at the umbilical cord, blocked/permeabilized for 3 hours in PBSMT (PBS+ 0.5% Triton X-100 +2% nonfat milk). Following the addition of 5 μg/ml rat anti-mouse PECAM1 antibody (Pharmingen), samples were incubated overnight at 4°C. Tissues were washed six times in PBSMT and incubated overnight in PBSMT+1:50 anti-rat Ig HRP-conjugate (Pharmingen). HRP staining was performed as previously described (Urness et al., 2000). Tissues were postfixed in 4% paraformaldehyde overnight at 4°C, cleared in 80% glycerol and photographed on a Leica MZ12 stereoscope equipped with a Zeiss Axiocam digital camera.

Hypoxia assay

Pregnant females (30 g) were injected IP with 200 ml of pimonidazole ('Hypoxyprobe' 10 mg/ml in PBS, Chemicon). After 2 hours, mice were killed by cervical dislocation, the embryos were dissected into 4% formaldehyde and the yolk sacs removed for genotyping. Following 16 hours fixation, embryos were serially dehydrated in ethanol, followed by xylene, embedded in paraffin and stored at 4°C. Sections (10 μm) were mounted on glass slides and stained with monoclonal antibodies directed against pimonidazole under conditions provided by the manufacturer. Primary antibody was diluted 200-fold; peroxidase staining for the secondary antibody was for 2 minutes at room temperature. Sections were counterstained with Mayer's hematoxylin prior to photography.

mRNA detection

Whole-mount in situ hybridization was performed as described previously (Urness et al., 2000). Embryos were harvested at E11.5. Decidual tissue was trimmed away and yolk sac fragments were collected from each embryo for genotyping. Placentas were fixed overnight at 4°C in 4% formaldehyde, pH 7.4. Antisense digoxigenin-labeled riboprobe was generated from

mouse *Unc5b* DNA using a DIG RNA Labeling Kit (Roche). In situ hybridization was performed overnight at 65°C with rotation in a Hybaid hybridization oven. All comparisons were between sibling pairs.

Tetraploid aggregation

Eight-week old C57Bl6/J mice were superovulated with 5 IU pregnant mares' serum gonadotropin followed after 48 hours with 5 IU human chorionic gonatotropin (hCG); mating with C57Bl6/J males immediately followed the hCG injection. Two-cell stage embryos were flushed at 1.5 days post plug, washed through two drops of M2 medium, four drops of mannitol and fused in mannitol using a Biological Laboratory Equipment BLS CF-150/B Cell Fusion apparatus. Settings were as follows: 40 V, 40 mseconds, enable 1.0. Following fusion, embryos were washed through three drops M2, three drops KSOM (Chemicon) and incubated in a 37° C CO_2 incubator. Most two-cell embryos fused to one cell within 10 minutes. Fused embryos were incubated in KSOM under oil overnight. Morulae (2.5-day old) were flushed from superovulated *Unc5b*$^{+/-}$ mice (mated with *Unc5b*$^{+/-}$ males), washed through Tyrode's (Sigma) to remove the zona pellucida, then washed through three drops M2 medium and three drops KSOM medium. One morula and one fused tetraploid embryo (now four-cell stage) were transferred into each miniwell of KSOM under oil, and incubated overnight. After 16 hours, all miniwells contained one fused blastocyst, which was implanted into 2.5-day pseudopregnant females (C57Bl6/J × CBA F1). Embryos were dissected and analyzed at E13.5.

Echocardiography

Embryos were analyzed and imaged noninvasively in utero using ultrasound biomicroscopy (UBS, Visualsonic Vevo 660) with a 40 MHz transducer and image-guided 23 MHz spectral pulsed-wave (PW) Doppler. Heart rate, blood flow velocities and blood flow volumes were determined from pulsed Doppler waveforms. During scanning, maternal body temperature and heart rate were maintained within normal range, and the duration of anesthesia was less than 1.5 hours (Mu and Adamson, 2006). The hemodynamics of embryos were measured every 6 hours for 36 hours, by which time all of the *Unc5b*-deficient embryos would have died. During each scan, the bladder was used as a reference for the midpoint between the left horn and the right horn of the fallopian uterus, and the relative location of embryos was mapped within the abdomen. After scanning at the final timepoint, a laparotomy was performed and the embryos were scanned a final time to correlate the order of embryo location by ultrasound with anatomic position. The genotype of embryos from previous scans was deduced from the location of embryos relative to each other, especially relative to the location of dead embryos. To confirm correlation between flow reversal and mutant genotype, a number of litters were scanned only until embryos with reversed diastolic flow in the umbilical artery were identified, at which time laparotomy was performed, anatomic correlation was established, and the embryos genotyped.

Umbilical vessel angiogenesis assays

Quantitative three-dimensional umbilical vessel angiogenesis assays were performed according to published methods (Nicosia et al., 2005) with minor modifications. Umbilical cord sections from murine embryos from *Unc5b*$^{+/-}$ × *Unc5b*$^{+/-}$ matings were harvested at E10.5. Immediately prior to harvest, three-dimensional collagen gels (0.25 ml/well) consisting of 2 mg/ml purified rat tail collagen I (Trevigen), 2.34 mg/ml $NaHCO_3$ in 2× concentrated EBM-2 (Lonza) medium supplemented with 1 μg/ml ascorbic acid and 0.2 μg/ml hydrocortisone with or without 100 ng/ml rmNetrin-1 (R&D Systems) were cast into the center wells of four-well chambered coverglasses (Nunclon) and stored on blue ice blocks to delay polymerization. Each embryo was sterilely dissected in the supplemented EBM-2 medium. A 0.5 mm fragment of yolk sac was retained in lysis buffer (50 mM KCl, 2.5 mM $MgCl_2$, 10 mM

Tris-HCl pH 8.5, 0.005% NP-40, 0.05% Tween 20, 0.01% gelatin) for PCR genotyping, and a 1.5 mm section of umbilical vessel (equidistant from placenta and embryo) was dissected and washed in EBM-2 (supplemented as above) prior to plating/polymerizing into the collagen gel. Gels with umbilical vessel explants were polymerized for 30 minutes at 37°C/5% CO_2, and subsequently overlaid with 0.25 ml of the supplemented EBM-2 medium. The following morning the medium was exchanged, and the explants photographed in phase-contrast on a Zeiss Axiovert inverted microscope equipped with a Zeiss Axiocam digital camera to confirm location and condition of the umbilical vessel explants. Thereafter, the medium was exchanged every 3–4 days, and the cultures were re-photographed on the tenth day of culture. The capillary outgrowths observed around the perimeter of each umbilical vessel photograph were counted, and data presented as the average number of capillary outgrowths per umbilical vessel perimeter. The experiment was performed six times on a total of 36 wild-type and 32 mutant siblings.

Embryo raising and MO injection experiments

Heterozygous Tg*(fli1:egfp)*^{y1} transgenic carriers (Lawson and Weinstein, 2002) were incrossed, and embryos were raised at 28.5°C in E2/GN embryo medium with 0.003% phenylthiourea to inhibit pigment formation and staged by time and overall morphology (Kimmel, 1995). *Unc5b* morphants typically reached the 48 hpf stage 1–2 hours after controls. Three MOs were obtained from Gene Tools: control MO ('standard control'), 5′-CCTCTTACCTCAGTTACAATTTATA-3′; *unc5b*SBMO1 (Lu et al., 2004), 5′-CATTTAACCGGCTCGTACCTGCATG-3′, which binds to 7 bp of exon 1 and 18 bp of intron 1; and *unc5b*SBMO2, 5′-AGGAAGACAATACAGCACCTCAGCA-3′, which binds to 7 bp of exon 4 and 18 bp of intron 4. MOs were diluted, stored and injected at 1 nl nominal volume as described previously (Wilson et al., 2006). RT-PCR was carried out as described previously (Wilson et al., 2006); primer sequences available upon request.

Microscopy and image analysis

fli:egfp-positive embryos were either imaged live or fixed and stained with anti-GFP before imaging (Wilson et al., 2006). Briefly, embryos were mounted laterally in agarose, right side down and confocal *z*-stacks were taken at the level of somites 7–12. *Z*-stacks were used to score the presence of PAVs in four to six hemisegments. We modified our analysis slightly by scoring only the near (right) side of the trunk, which could be imaged most clearly; and by calculating in each embryo the fraction of hemisegments with absent, partial or complete PAVs, then averaging these fractions across embryos. Statistical analysis used two-tailed Mann-Whitney tests (Instat3, Graphpad).

RESULTS

Endothelial restricted ablation of Unc5b causes embryonic lethality

Because of the broad expression pattern of *Unc5b* in the murine embryo, we generated an allele of *Unc5b* (Wilson et al., 2006) that can be inactivated, conditionally, through tissue-restricted expression of CRE recombinase. This allele, *Unc5b*^{flox}, contains *loxP* sites within introns 3 and 13. CRE-mediated deletion of the intervening sequences removes much of the ligand-binding domain, the entire transmembrane domain, and most of the cytoplasmic signaling domain of the mature protein, generating a presumed null allele. To reduce the chance of cis-acting effects, the selectable marker gene used in construction of this allele was removed prior to analysis. We also engineered mice that transmit the deletion allele, *Unc5b*$^{-}$, through the germline. Mice homozygous for this mutation die in utero between 12 and 13.5 days post-fertilization (E12–E13.5). Our preliminary phenotypic characterization of *Unc5b*$^{-/-}$ embryos has been described (Wilson et al., 2006) and, surprisingly, it revealed none of the excessive vascular sprouting described by Lu et al. (Lu et al., 2004).

To systematically inactivate *Unc5b* in a tissue-specific fashion, animals homozygous for the conditional allele (*Unc5b*$^{flox/flox}$) were mated with animals heterozygous for the *Unc5b* null allele (*Unc5b*$^{+/-}$) and carrying one of a variety of *Cre* genes under tissue-restricted control. Deletion of *Unc5b* in neural crest-derived tissues [*Wnt1-Cre* (Jiang et al., 2000)], smooth and cardiac muscle [*Tag1n-Cre* (Holtwick et al., 2002)] in the nervous system [*Nestin1-Cre* (Sclafani et al., 2006)] or in hematopoietic lineages [*Vav1-Cre* (Stadtfeld and Graf, 2005)] resulted in mice that survived to adulthood and that appeared normal (Table 1 and data not shown). When *Unc5b* was deleted by an endothelial-expressed *Cre* transgene, *Tie2-Cre* (Kisanuki et al., 2001), however, no animals of the genotype *Unc5b*$^{-/flox}$; +/*Tg(Tie2-Cre)*, were ever recovered at birth. Embryos of this genotype died in mid-gestation between 12 and 13.5 days post-fertilization and were indistinguishable from homozygous null *Unc5b*$^{-/-}$ embryos (data not shown). The implication from these results is that vascular expression, and only vascular expression, of *Unc5b* is required for viability.

Arteriole reduction in *Unc5b*-deficient placentas

Embryonic death in the E10–E13 period is generally attributed to failures in cardiac function, hematopoiesis or placentation (Papaioannou and Behringer, 2005), and *Tie2-Cre* is expressed in these relevant tissues (Kisanuki et al., 2001). Histological analyses of E12.5 embryos revealed no differences in heart structure or in the morphology of coronary vessels between *Unc5b*$^{+/flox}$; +/*Tg(Tie2-Cre)* and *Unc5b*$^{-/flox}$; +/*Tg(Tie2-Cre)* embryos; blood counts were equivalent, as was the profile of circulating cells; and the vasculature of the somites, neural tube, yolk sac and hindbrain were indistinguishable (data not shown). The only discernible difference between the two genotypes was within the placental labyrinth: fetal-derived arterioles, visualized either by smooth muscle or endothelial specific stains, were less numerous in embryos lacking vascular *Unc5b* (Fig. 1).

Defective umbilical blood flow and hypoxia in *Unc5b*-deficient embryos

To determine the functional relevance of this placental defect, Doppler flow analysis was performed on umbilical vessels in utero. Three pregnancies from *Unc5b*$^{flox/flox}$ × *Unc5b*$^{+/-}$; *Tg(Tie2-Cre)/Tg(Tie2-Cre)* crosses were probed at regular intervals from E11.0 to E13.5. At these time points, normal umbilical artery flow is predominantly systolic with a minimal amount of flow in diastole. Beginning at ~E12.0, significant and reversed blood flow in diastole within the umbilical arteries of mutant embryos could be detected in some embryos (Fig. 2A, Table 2A). As pregnancy proceeded, the number of embryos with abnormal flow increased, as did the degree of flow reversal (e.g. −22% to −91%, Fig. 2A). By E13.5, all embryos that had exhibited reversed flow were dead. In another set of identical crosses, embryos were probed at a single time point, E12.5, and subsequently killed and genotyped (Fig. 2B,C). There was a strong genotype/phenotype correlation between the vascular deletion of *Unc5b* and flow reversal. Umbilical artery diastolic flow reversal is a clinical sign of fetal distress and is consistent with an abnormally high resistance within the placenta, a plausible consequence of the reduced number of arterioles. Consistent with this interpretation, physiological and anatomical changes in cardiac function, such as bradycardia and pericardial effusion, were only detected after the onset of umbilical arterial flow reversal and immediately prior to death (Fig. 2A) but not earlier (Fig. 2C).

By E13, the embryo is nutritionally dependent on maternal blood. We thus hypothesized that the defective placenta and the accompanying circulatory abnormality would result in a decrease in available metabolites. As a metabolic indicator, O_2 levels of embryos were assessed by examining the ability of tissues to retain pimonidazole, a compound that shows enhanced protein-binding capacity under hypoxic conditions (Raleigh et al., 1987). At 12.5 days after fertilization, pregnant females were injected with pimonidazole. Two hours later, embryos were removed and apparently viable, outwardly normal, embryos were fixed and sectioned.

Bound pimonidazole was then assessed by immunostaining. At E12.5, the majority (4/5) of *Unc5b*$^{-/-}$ embryos exhibited a higher level of pimonidazole immunoreactivity than did their wild-type counterparts (Fig. 2D,E), suggestive of a hypoxic environment and implying a direct link between altered umbilical flow and ultimate death.

UNC5B acts within the embryo proper

The arterioles affected by *Unc5b* loss are derived from the umbilical vessels emanating from the embryo proper, but their patterning depends on signaling from the adjacent extra-embryonic trophoblast (Adamson et al., 2002; Cross et al., 2003; Rinkenberger and Werb, 2000; Rossant and Cross, 2001). To understand more specifically the requirement for *Unc5b*, we examined its gene expression in the placenta. Sections of E12.0 placentas of genotypes *Unc5b*$^{+/flox}$; +/*Tg(Tie2-Cre)*; and *Unc5b*$^{-/flox}$; +/*Tg(Tie2-Cre)* were probed with RNA complementary to *Unc5b* mRNA. As shown in Fig. 3A,B, binding of this probe was restricted to the labyrinth but could not be detected in placentas in which *Unc5b* had been deleted by endothelial-expressed CRE (Fig. 3A,B). Thus, placental expression of UNC5B is limited to the fetal-derived endothelium. These data suggest a model whereby UNC5B-expressing endothelial cells within the labyrinth respond to signals emanating from the trophectoderm and direct proper vascular development. Consistent with this idea, expression of the secreted guidance factor, netrin 1, an UNC5B ligand, can be detected in the trophoblast giant cells (Fig. 3C,D). Although no placental phenotype has been described in mice deficient for netrin 1 (Salminen et al., 2000; Serafini et al., 1996), the mutations analyzed in those studies were hypomorphic alleles that synthesize detectable levels of wild-type transcript.

This model also predicts that wild-type trophoblast cells should be unable to rescue embryos deficient in *Unc5b* (Nagy et al., 1993). To test this prediction, we aggregated diploid morulae from an *Unc5b*$^{+/-}$ intercross with tetraploid, wild-type, two-cell stage embryos that can contribute only to the extra-embryonic tissues (Nagy et al., 1993). Fused embryos were implanted into foster mothers, harvested at E13.5 and examined for viability and genotype. As summarized in Table 2B, all wild-type and heterozygous embryos were viable, whereas 11/12 *Unc5b*$^{-/-}$ embryos were dead. Examination by PCR of genomic DNA isolated from extra-embryonic tissue of the *Unc5b*$^{-/-}$ embryos showed a significant contribution from wild-type (tetraploid) cells (data not shown). The fact that these cells were incapable of supporting an *Unc5b* mutant embryo implies that the deficiencies resulting from this genotype are within the embryo proper.

Evidence that UNC5B is active within the fetal-placental vasculature was provided by examining the growth of isolated umbilical arteries in vitro. When cultured on a collagen matrix in the absence of serum, umbilical arterial explants isolated from *Unc5b*$^{+/+}$ embryos support a more vigorous netrin 1-dependent outgrowth than do those isolated from their *Unc5b*$^{-/-}$ littermates (Fig. 3E,F).

Knock-down of Unc5b inhibits PAV formation in zebrafish

The role of netrin signaling in zebrafish vascular development is not without controversy. During development of the embryonic trunk vasculature, the zebrafish netrin 1 ortholog, *netrin1a*, is expressed at the horizontal myoseptum (Lauderdale et al., 1997; Wilson et al., 2006), precisely where secondary sprouts growing dorsally from the posterior cardinal vein (PCV) grow laterally and turn anteroposteriorly to form the parachordal vessel (PAV). It has been reported that knocking down either *netrin1a* or *unc5b* using antisense morpholino oligonucleotides (MOs) disrupts intersomitic vessel (ISV) formation and leads to excess vessel branching (Lu et al., 2004). We found, however, that a carefully titrated dose of a splice-blocking MO against *netrin1a* led to a highly penetrant phenotype in which the PAV failed to

form (Wilson et al., 2006). ISVs are only very rarely affected at this dose, and overall trunk morphology appears normal, unlike that seen at higher doses (A.S. and C.-B.C., unpublished).

We therefore reexamined formation of the trunk vasculature after *unc5b* knockdown, injecting two different MOs against *unc5b: unc5b*SBMO1 [identical to that used by Lu et al. (Lu et al., 2004)] and *unc5b*SBMO2, and using the *fli:egfp* transgene to visualize endothelial cells (Fig. 4). In preliminary dose-response experiments, we chose MO doses (1 ng *unc5b*SBMO1 or 4 ng *unc5b*SBMO2) that yielded embryos with normal trunk morphology (Fig. 4A–D). This was crucial as, even at moderate doses (1.5 ng), *unc5b*SBMO1 caused gross morphological defects (strongly curved tails, hindbrain edema and small eyes), which may reflect off-target effects. At these doses, both MOs were effective, as shown by significant reductions in wild-type *unc5b* mRNA detected by RT-PCR (see Fig. S1 in the supplementary material). Although development of the overall vasculature was normal, including the dorsal aorta, PCV and ISVs, we saw a specific, highly penetrant effect on PAV formation (Fig. 4E–H). PAVs normally form by ~36 hpf. To avoid potential confounding effects of mild developmental delay, we scored PAVs at 48 hpf. The fraction of hemisegments that completely lacked a PAV increased from 1±1% to 46±6% (mean±s.e.m., $P<0.0001$) with *unc5b*SBMO1, and from 2±2% to 70±7% ($P<0.0001$) with *unc5b*SBMO2 (Fig. 4I,J). The concordant results with two nonoverlapping MOs strongly suggests that the lack of PAVs is specifically due to loss of *unc5b* function, rather than an off-target effect. Given the expression of *netrin1a* at the horizontal myoseptum, the most parsimonious explanation is that Ntn1a-Unc5b signaling is pro-angiogenic in this system.

DISCUSSION

We have analyzed the developmental consequences of *Unc5b* mutagenesis in both mouse and zebrafish. Deletion of *Unc5b* within the endothelial cells – and only within the endothelial cells – of the developing murine vasculature leads to a mid-gestational lethality that phenocopies universal ablation of *Unc5b*. The only observed defect in embryos lacking *Unc5b* is a reduction in the number of labyrinthine arterioles within the placenta. This leads to an increase in placental resistance, followed by flow reversal in the umbilical artery, hypoxia, cardiac failure and ultimately death. Morphological analyses of mutant embryos revealed no other defects, and fetal echocardiography showed no signs of high-output or low-output heart failure or lethal arrhythmia predating the onset of structural and physiological placental abnormalities. The reduction in the number of placental arterioles in the absence of *Unc5b* implies a pro-angiogenic role for netrin/UNC5B signaling during development, which is further supported by our observation that umbilical arteries isolated from *Unc5b*-deficient embryos were unable to support vessel outgrowth in vitro. A pro-angiogenic role of UNC5B was also observed in the zebrafish trunk vasculature, where we found that the knockdown of *unc5b* function, using carefully titrated doses of two different MOs, leads to a specific and highly penetrant absence of PAVs. Although we cannot rule out the possibility that UNC5B may play some role in ISV formation that would be revealed by higher doses of MO (Lu et al., 2004), we did not analyze higher doses because of morphological defects that were potentially nonspecific. This issue would be best addressed by isolating mutant alleles for *unc5b*. Furthermore, we note that the morphant images of Lu et al. (Lu et al., 2004) appear to show missing PAVs in some segments; in other segments, secondary sprouts appear to turn normally to form the PAV, but have been interpreted as increased vessel branching. Together with the observations that the PAV forms along the muscle pioneer cells that line the horizontal myoseptum and express *netrin1a*, and that *netrin1a* morphants have very similar phenotypes to *unc5b* morphants (Wilson et al., 2006), these data support an important pro-angiogenic role for Ntn1a/Unc5b signaling in zebrafish lymphatic development.

Though zebrafish do not have placental arterioles and mice do not have a structural equivalent to the PAV, our developmental studies indicate that netrin signaling has evolved to ensure the formation of specific subsets of vessels. Thus, in contrast to VEGF signaling, which has profound effects on virtually all endothelial cells and vascular beds during developmental angiogenesis (Ferrara et al., 2003), guidance cues in general and UNC5B specifically, may provide an additional level of regulation to coordinate the spatial and temporal organization of tissue-specific vascular beds during embryogenesis. Because the first vital requirement for UNC5B is during mid-gestation, the reagents used in this study were unable to ascertain a function in later stages of development or within the adult. Such an assessment requires the use of alternative mutagenesis schemes, which we are vigorously pursuing.

A role for UNC5B in embryonic angiogenesis was originally postulated because of its vascular-specific expression pattern and was supported by the characterization of a mouse mutant in which exons 3 and 4 of *Unc5b* were replaced with 8 kb of exogenous DNA encoding the *lacZ* and alkaline phosphatase genes (Lu et al., 2004). Although embryos homozygous for that allele died at the same time as those containing the exon3-13 deletion allele described in our previous work (Wilson et al., 2006) and in this manuscript, they were characterized as having increased capillary branching in the embryo proper, which the authors hypothesized would raise vascular resistance and precipitate heart failure. However, this study did not report physiological measurements of embryonic cardiac function or any analyses – functional or morphological – of the placenta. It would be interesting to re-examine this allele in the light of our present findings.

The placenta is one of the more complex vascularized tissues in mammals. It is derived from three distinct sources: maternal tissue, extra-embryonic fetal tissue, and arteries and veins originating from the embryo proper. The fetal-placental vascular system circulates fetal blood and interdigitates with the trophoblast sinuses filled with maternal blood (Cross, 2005; Red-Horse et al., 2004). Assembly of the vasculature within the placental labyrinth requires signaling between the extra-embryonic tissue and the fetal-placental vessels. Mutational analysis has revealed dozens of genes required for this communication, with virtually all reports concluding that these genes exert their effects through the extra-embryonic trophectoderm (Cross, 2005; Rossant and Cross, 2001). In fact, patterning by the trophoblast cells is deemed an essential guide for proper growth of the fetal vessels into and within the labyrinth layer. The specific and autonomous role of *Unc5b* in promoting fetal-placental arteriogenesis emphasizes that vascular signaling pathways on the fetal-placental side of the equation should not be ignored. As the UNC5B-deficient phenotype could not be rescued by a wild-type trophectoderm, we propose that UNC5B-mediated signaling is a specific and autonomous component of fetal-placental angiogenesis, and that *Unc5b* disruption represents a rare, if not the first, example of a mutation acting solely with the fetal placental vasculature.

Abnormal placental vascular development may be etiologically linked to multiple obstetric complications, including early pregnancy loss, intrauterine growth restriction, fetal death and pre-eclampsia, and may have lasting consequences for childhood development (Cross, 2006; Mayhew et al., 2007; Redman and Sargent, 2003). Recent studies have assigned a role for maternal angiogenic signaling pathways in pre-eclampsia (Levine et al., 2006; Wallner et al., 2007). The findings presented herein provide genetic evidence that defects in netrin/UNC5B signaling, which disrupts the fetal contribution to the placental vasculature, should be considered in the pathogenesis of clinical syndromes of uteroplacental insufficiency (Cross, 2003; Levine et al., 2006; Wallner et al., 2007).

Acknowledgements

We thank the many former and current Li and Chien laboratory members for their support with this project; Diana Lim for help in manuscript preparation; Antonio Frias, Suzanne Mansour, Shannon Odelberg and L. Charles Murtaugh for critique of the manuscript; Antonio Frias for insights into uteroplacental insufficiency; the University of Utah Mouse Core laboratory for assistance with tetraploid aggregation; and Philippe Soriano, Matthias Stadtfeld, Masashi Yanagisawa and Lindsay Hinck for mouse strains. This work was supported by grants to D.Y.L. from the NIH, American Cancer Society, American Heart Association, Flight Attendants Medical Research Institute and the Burroughs Wellcome Fund and by RO1 EY12873 to C.-B.C.

References

Adamson SL, Lu Y, Whiteley KJ, Holmyard D, Hemberger M, Pfarrer C, Cross JC. Interactions between trophoblast cells and the maternal and fetal circulation in the mouse placenta. Dev Biol 2002;250:358–373. [PubMed: 12376109]

Cirulli V, Yebra M. Netrins: beyond the brain. Nat Rev Mol Cell Biol 2007;8:296–306. [PubMed: 17356579]

Cross JC. The genetics of pre-eclampsia: a feto-placental or maternal problem? Clin Genet 2003;64:96–103. [PubMed: 12859402]

Cross JC. How to make a placenta: mechanisms of trophoblast cell differentiation in mice – a review. Placenta Suppl 2005;26:S3–S9.

Cross JC. Placental function in development and disease. Reprod Fertil Dev 2006;18:71–76. [PubMed: 16478604]

Cross JC, Baczyk D, Dobric N, Hemberger M, Hughes M, Simmons DG, Yamamoto H, Kingdom JC. Genes, development and evolution of the placenta. Placenta 2003;24:123–130. [PubMed: 12596737]

Engelkamp D. Cloning of three mouse Unc5 genes and their expression patterns at mid-gestation. Mech Dev 2002;118:191–197. [PubMed: 12351186]

Ferrara N, Gerber HP, LeCouter J. The biology of VEGF and its receptors. Nat Med 2003;9:669–676. [PubMed: 12778165]

Holtwick R, Gotthardt M, Skryabin B, Steinmetz M, Potthast R, Zetsche B, Hammer RE, Herz J, Kuhn M. Smooth muscle-selective deletion of guanylyl cyclase-A prevents the acute but not chronic effects of ANP on blood pressure. Proc Natl Acad Sci USA 2002;99:7142–7147. [PubMed: 11997476]

Huber AB, Kolodkin AL, Ginty DD, Cloutier JF. Signaling at the growth cone: ligand-receptor complexes and the control of axon growth and guidance. Annu Rev Neurosci 2003;26:509–563. [PubMed: 12677003]

Jiang X, Rowitch DH, Soriano P, McMahon AP, Sucov HM. Fate of the mammalian cardiac neural crest. Development 2000;127:1607–1616. [PubMed: 10725237]

Kennedy TE, Serafini T, de la Torre JR, Tessier-Lavigne M. Netrins are diffusible chemotropic factors for commissural axons in the embryonic spinal cord. Cell 1994;78:425–435. [PubMed: 8062385]

Kimmel CB, Ballard WW, Kimmel SR, Ullmann B, Schilling TF. Stages of embryonic development of the zebrafish. Dev Dyn 1995;203:253–310. [PubMed: 8589427]

Kisanuki YY, Hammer RE, Miyazaki J, Williams SC, Richardson JA, Yanagisawa M. Tie2-Cre transgenic mice: a new model for endothelial cell-lineage analysis in vivo. Dev Biol 2001;230:230–242. [PubMed: 11161575]

Lauderdale JD, Davis NM, Kuwada JY. Axon tracts correlate with netrin-1a expression in the zebrafish embryo. Mol Cell Neurosci 1997;9:293–313. [PubMed: 9268507]

Lawson ND, Weinstein BM. In vivo imaging of embryonic vascular development using transgenic zebrafish. Dev Biol 2002;248:307–318. [PubMed: 12167406]

Leonardo ED, Hinck L, Masu M, Keino-Masu K, Ackerman SL, Tessier-Lavigne M. Vertebrate homologues of C. elegans UNC-5 are candidate netrin receptors. Nature 1997;386:833–838. [PubMed: 9126742]

Levine RJ, Lam C, Qian C, Yu KF, Maynard SE, Sachs BP, Sibai BM, Epstein FH, Romero R, Thadhani R, et al. Soluble endoglin and other circulating antiangiogenic factors in preeclampsia. N Engl J Med 2006;355:992–1005. [PubMed: 16957146]

Lu X, Le Noble F, Yuan L, Jiang Q, De Lafarge B, Sugiyama D, Breant C, Claes F, De Smet F, Thomas JL, et al. The netrin receptor UNC5B mediates guidance events controlling morphogenesis of the vascular system. Nature 2004;432:179–186. [PubMed: 15510105]

Mayhew TM, Manwani R, Ohadike C, Wijesekara J, Baker PN. The placenta in pre-eclampsia and intrauterine growth restriction: studies on exchange surface areas, diffusion distances and villous membrane diffusive conductances. Placenta 2007;28:233–238. [PubMed: 16635527]

Mu J, Adamson SL. Developmental changes in hemodynamics of uterine artery, utero- and umbilicoplacental, and vitelline circulations in mouse throughout gestation. Am J Physiol Heart Circ Physiol 2006;291:H1421–H1428. [PubMed: 16603699]

Nagy A, Rossant J, Nagy R, Abramow-Newerly W, Roder JC. Derivation of completely cell culture-derived mice from early-passage embryonic stem cells. Proc Natl Acad Sci USA 1993;90:8424–8428. [PubMed: 8378314]

Nguyen A, Cai H. Netrin-1 induces angiogenesis via a DCC-dependent ERK1/2-eNOS feed-forward mechanism. Proc Natl Acad Sci USA 2006;103:6530–6535. [PubMed: 16611730]

Nicosia RF, Zhu WH, Fogel E, Howson KM, Aplin AC. A new ex vivo model to study venous angiogenesis and arterio-venous anastomosis formation. J Vasc Res 2005;42:111–119. [PubMed: 15665546]

Papaioannou, VE.; Behringer, RR. Mouse Phenotypes. Cold Spring Harbor, NY: Cold Spring Harbor Laboratory Press; 2005.

Park KW, Crouse D, Lee M, Karnik SK, Sorensen LK, Murphy KJ, Kuo CJ, Li DY. The axonal attractant Netrin-1 is an angiogenic factor. Proc Natl Acad Sci USA 2004;101:16210–16215. [PubMed: 15520390]

Raleigh JA, Miller GG, Franko AJ, Koch CJ, Fuciarelli AF, Kelly DA. Fluorescence immunohistochemical detection of hypoxic cells in spheroids and tumours. Br J Cancer 1987;56:395–400. [PubMed: 3689657]

Red-Horse K, Zhou Y, Genbacev O, Prakobphol A, Foulk R, McMaster M, Fisher SJ. Trophoblast differentiation during embryo implantation and formation of the maternal-fetal interface. J Clin Invest 2004;114:744–754. [PubMed: 15372095]

Redman CW, Sargent IL. Pre-eclampsia, the placenta and the maternal systemic inflammatory response-a review. Placenta Suppl 2003;24:S21–S27.

Rinkenberger J, Werb Z. The labyrinthine placenta. Nat Genet 2000;25:248–250. [PubMed: 10888863]

Rossant J, Cross JC. Placental development: lessons from mouse mutants. Nat Rev Genet 2001;2:538–548. [PubMed: 11433360]

Salminen M, Meyer BI, Bober E, Gruss P. Netrin 1 is required for semicircular canal formation in the mouse inner ear. Development 2000;127:13–22. [PubMed: 10654596]

Sclafani AM, Skidmore JM, Ramaprakash H, Trumpp A, Gage PJ, Martin DM. Nestin-Cre mediated deletion of Pitx2 in the mouse. Genesis 2006;44:336–344. [PubMed: 16823861]

Serafini T, Kennedy TE, Galko MJ, Mirzayan C, Jessell TM, Tessier-Lavigne M. The netrins define a family of axon outgrowth-promoting proteins homologous to C. elegans UNC-6. Cell 1994;78:409–424. [PubMed: 8062384]

Serafini T, Colamarino SA, Leonardo ED, Wang H, Beddington R, Skarnes WC, Tessier-Lavigne M. Netrin-1 is required for commissural axon guidance in the developing vertebrate nervous system. Cell 1996;87:1001–1014. [PubMed: 8978605]

Soriano P. Generalized lacZ expression with the ROSA26 Cre reporter strain. Nat Genet 1999;21:70–71. [PubMed: 9916792]

Stadtfeld M, Graf T. Assessing the role of hematopoietic plasticity for endothelial and hepatocyte development by non-invasive lineage tracing. Development 2005;132:203–213. [PubMed: 15576407]

Tessier-Lavigne M, Goodman CS. The molecular biology of axon guidance. Science 1996;274:1123–1133. [PubMed: 8895455]

Urness LD, Sorensen LK, Li DY. Arteriovenous malformations in mice lacking activin receptor-like kinase-1. Nat Genet 2000;26:328–331. [PubMed: 11062473]

Wallner W, Sengenberger R, Strick R, Strissel PL, Meurer B, Beckmann MW, Schlembach D. Angiogenic growth factors in maternal and fetal serum in pregnancies complicated by intrauterine growth restriction. Clin Sci 2007;112:51–57. [PubMed: 16928195]

Wilson BD, Ii M, Park KW, Suli A, Sorensen LK, Larrieu-Lahargue F, Urness LD, Suh W, Asai J, Kock GA, et al. Netrins promote developmental and therapeutic angiogenesis. Science 2006;313:640–644. [PubMed: 16809490]

Yaniv K, Isogai S, Castranova D, Dye L, Hitomi J, Weinstein BM. Live imaging of lymphatic development in the zebrafish. Nat Med 2006;12:711–716. [PubMed: 16732279]

Yebra M, Montgomery AM, Diaferia GR, Kaido T, Silletti S, Perez B, Just ML, Hildbrand S, Hurford R, Florkiewicz E, et al. Recognition of the neural chemoattractant Netrin-1 by integrins alpha6beta4 and alpha3beta1 regulates epithelial cell adhesion and migration. Dev Cell 2003;5:695–707. [PubMed: 14602071]

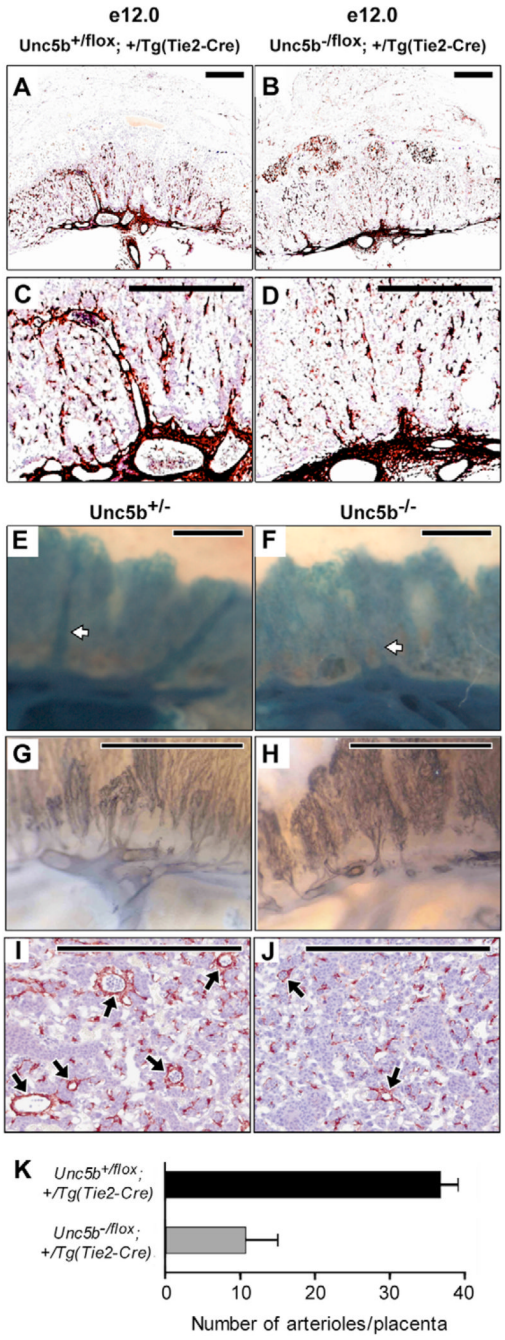

Fig. 1. Vascular ablation of Unc5b impacts labyrinthine arterioles

Embryos were harvested at E12.0 from *Unc5b*$^{flox/flox}$ × *Unc5b*$^{+/-}$; *Tg(Tie2-Cre)/Tg(Tie2-Cre)* (**A–D**), *Unc5b*$^{+/-}$*; R26R* [Rosa26 Reporter (Soriano, 1999)] × *Unc5b*$^{+/-}$; *Tg(Tie2-Cre)/Tg(Tie2-Cre)* (**E**,**F**) or *Unc5b*$^{+/-}$ × *Unc5b*$^{+/-}$ (**G–J**) matings. Placentas were dissected, formalin fixed, hemisected and stained for: smooth muscle actin (anti-smooth muscle actin antibody followed by HRP-conjugated secondary antibody) to identify smooth muscle cells surrounding the arterial bed (A–D); for β-galactosidase activity (X-gal) to identify endothelial expression of *Tie2-Cre* (E,F); and for Pecam l (anti-Pecam1 antibody followed by HRP-conjugated secondary antibody) to highlight the endothelium (G,H). There is a decrease in the number of robust vertical vessel stalks in placentas lacking UNC5B (B,D,F,H) when compared with their

littermate controls (A,C,E,G). This is also shown in I,J, which represent 10 μm cross-sections through samples stained for smooth muscle actin. Arterioles are indicated by arrows; scale bars: 0.5 mm. (**K**) The number of arterioles per placenta was determined by serial sectioning (10 μm) of hemisected placentas, staining for smooth muscle actin and visually counting all vessels. Paired littermates (three pairs) representing each of the two genotypes were used for all measurements. Error bars are standard deviation.

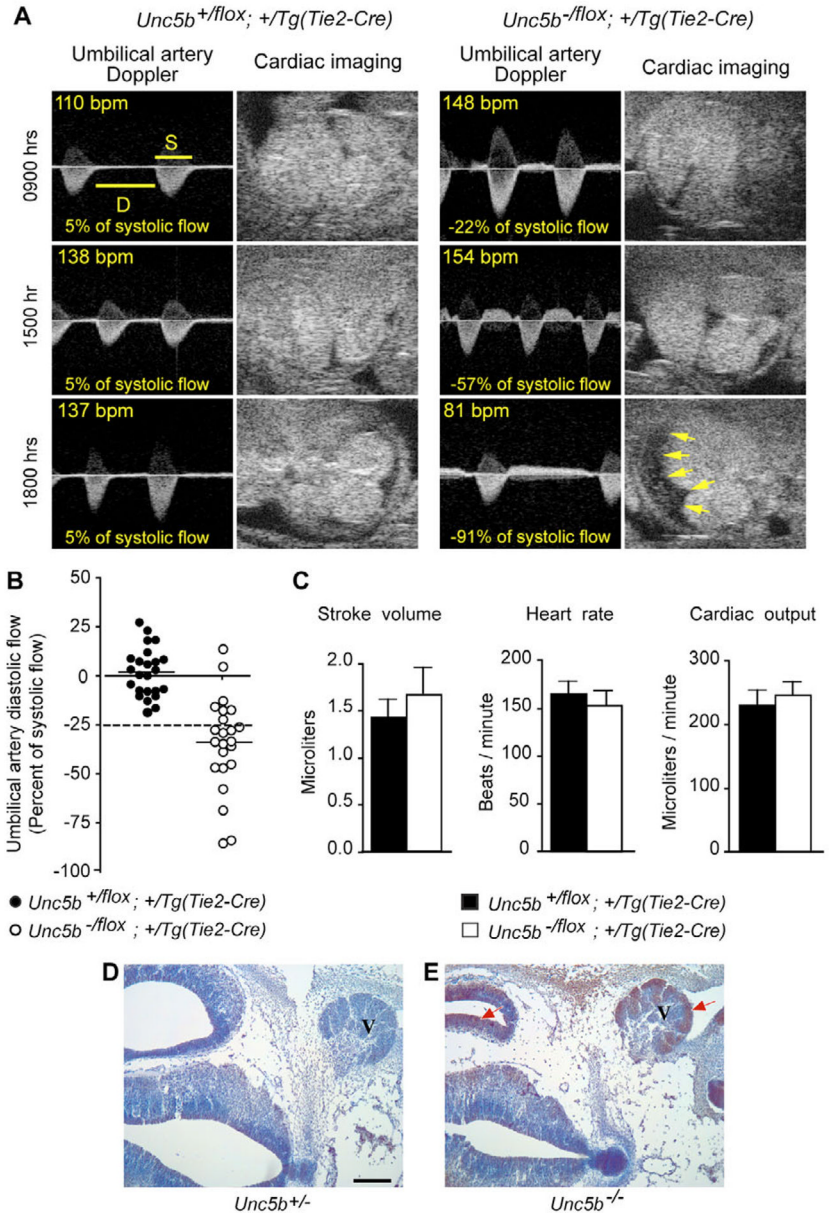

Fig. 2. Physiological assessment of embryos

(**A**) Doppler flow analysis of umbilical arteries and hearts in utero. For longitudinal follow-up of umbilical artery Doppler flow, *Unc5b*$^{+/flox}$; +/*Tg(Tie2-Cre)* and *Unc5b*$^{-/flox}$;+/*Tg(Tie2-Cre)* embryos were monitored on E12 at the time intervals indicated on the left. The ratio of diastolic (D) flow (time velocity integral) over systolic (S) flow is shown as a percentage with a negative number indicative of reverse flow. The ratio decreased progressively over time in the mutant embryo and preceded pericardial effusion (arrows) and bradycardia. (**B**) Quantitation of umbilical artery diastolic flow reversal. The ratio of umbilical diastolic flow (time velocity integral) over systolic flow was used to quantitate the degree of end diastolic reverse flow and the ratio of −25% of systolic flow (broken line) was chosen as a threshold for significant reversal; 24 *Unc5b*$^{+/flox}$; +/*Tg(Tie2-Cre)* and 23 *Unc5b*$^{-/flox}$;+/*Tg(Tie2-Cre)* embryos were sampled at a single time point at E12.5. (**C**) The stroke volume, heart rate and cardiac output were recorded at the onset of significant diastolic reverse flow; data from four

Unc5b$^{+/flox}$; +/*Tg(Tie2-Cre)* and three *Unc5b*$^{-/flox}$;+/*Tg(Tie2-Cre)* are reported; error bars are standard deviation. (**D**,**E**) Increased hypoxia in *Unc5b*$^{-/-}$ embryos. Pregnant females were injected with pimonidazole 2 hours prior to sacrifice and removal of embryos. Sections (10 μm) from the hindbrain region of E12.5 *Unc5b*$^{+/-}$ (D) and *Unc5b*$^{-/-}$ (E) embryos were probed with antibodies directed against pimonidazole and HRP-conjugated secondary antibodies, stained for HRP activity (brown, indicated by arrows) and counterstained with hematoxylin (blue). V, trigeminal ganglion. Scale bar: 100 μm.

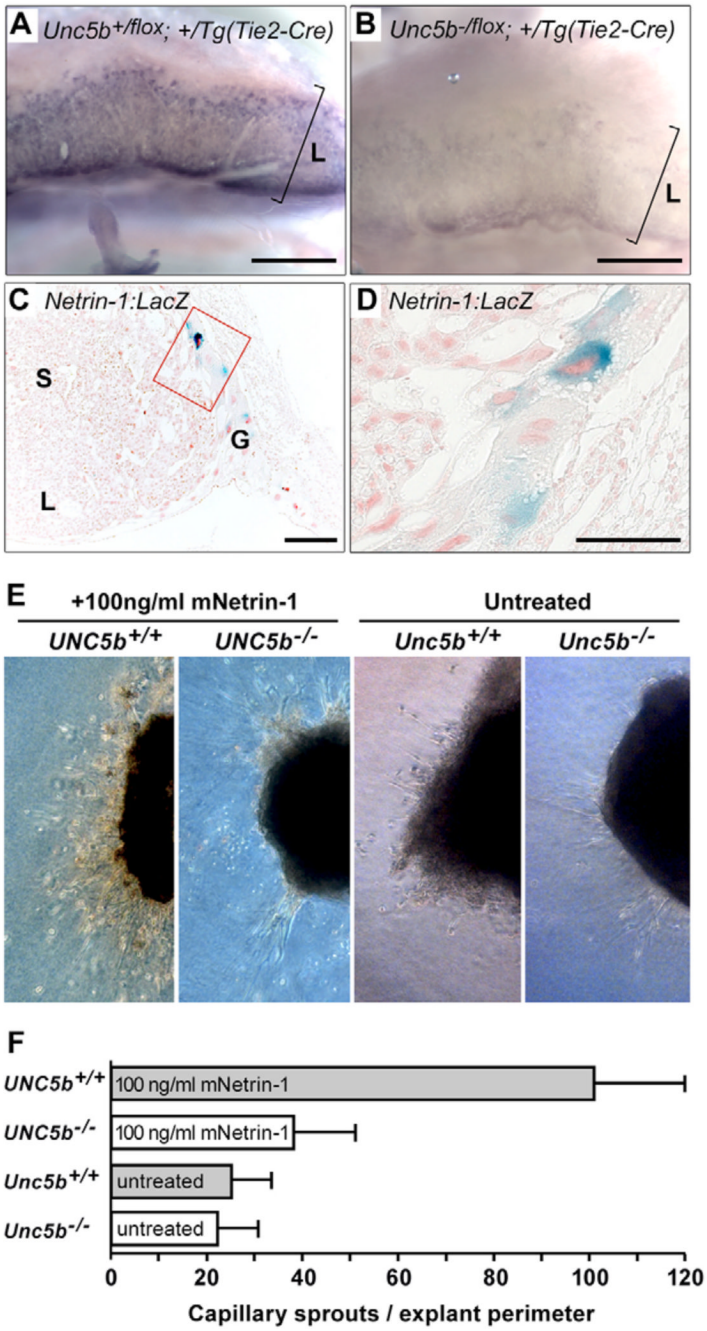

Fig. 3. Unc5b/Netrin signaling in the placenta

(**A**,**B**) *Unc5b* mRNA localization in the labyrinth. Placentas from E12.5 embryos were hemisected and probed with antisense RNA complementary to *Unc5b* mRNA. (A) *Unc5b*$^{+/flox}$;+/*Tg(Tie2-Cre)* and (B) *Unc5b*$^{-/flox}$; +/*Tg(Tie2-Cre)*; L indicates extent of labyrinthine layer. Scale bars: 1 mm. (**C**,**D**) Netrin expression in giant trophoblast cells. Placentas (E12.5) from embryos heterozygous for the *netrin1:lacZ* gene trap (Serafini et al., 1996) were fixed, hemisected and stained with X-gal to detect *lacZ* activity; 10 μm sections were mounted on slides and counterstained with nuclear Fast Red. L, labyrinth; S, spongiotrophoblast; G, giant trophoblast cell layer. Image in D is a 4 × magnification of boxed area in C. Scale bars: 200 μm in C; 100 μm in D. (**E**) Growth of umbilical vessels in vitro.

Umbilical vessels at E10.5 were explanted into collagen gels and allowed to sprout for 10 days in the presence or absence of netrin 1 protein. Numbers of sprouts were counted under phase contrast. Genotypes and growth conditions are indicated above each frame. (**F**) Quantitation from four pairs of umbilical arteries of each genotype. Error bars are standard deviation.

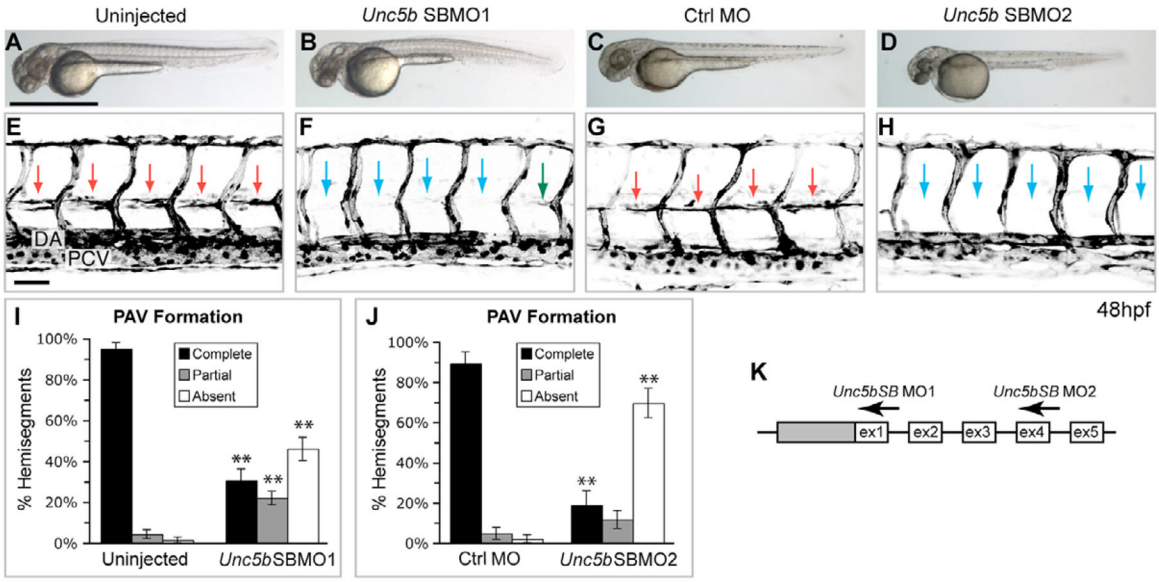

Fig. 4. Knockdown of zebrafish *unc5b* prevents formation of a specific vessel: the PAV

(**A–D**) Bright-field images of live embryos, anterior towards the left. Overall trunk morphology is normal in *unc5b* morphants (1 ng *unc5b*SBMO1 or 4 ng *unc5b*SBMO2) compared with controls (uninjected or 8 ng control MO). (**E–H**) Confocal projections of *fli:egfp* transgenics (reverse contrast) show that *unc5b* knockdown prevents PAV formation. Lateral views of somites 7–11, anterior towards the left; confocal projections through entire trunk. Embryos imaged live (G,H) or fixed after anti-GFP staining (E,F). (E,G) In uninjected embryos or control morphants at 48 hpf, almost every hemisegment is spanned by a PAV at the horizontal myoseptum (red arrows). (F,H) In embryos injected with either of two *unc5b* splice-blocking MOs, PAVs are absent (blue arrows) or only partially span their hemisegment (green arrows). DA, dorsal aorta; PCV, posterior cardinal vein. (**I**,**J**) PAV formation scored as percentage of hemisegments per embryo. In controls, at least 98% of hemisegments have complete or partial PAVs; this fraction is drastically reduced by either *unc5b* MO. *n*=25–30 embryos per condition; ***P*<0.0001. Bars show mean±s.e.m. (**K**) Partial *unc5b* genomic structure (not to scale), showing 5′ UTR (gray box), coding exons (white boxes) and MO targets. Scale bars: 1 mm in A for A–D; 50 μm in E for E–H.

Table 1

Tissue-specific deletion of Unc5b

Cross	$Unc5b^{flox/flox}$×$Unc5b^{+/-}$;+/*Tg(Tie2-Cre)*			
Genotype	$Unc5b^{-/flox}$;+/*Tg(Tie2-Cre)*	$Unc5b^{+/flox}$;+/*Tg(Tie2-Cre)*	$Unc5b^{-/flox}$	$Unc5b^{+/flox}$
Number of progeny	0	25	28	24
Cross	$Unc5b^{flox/flox}$×$Unc5b^{+/-}$;+/*Tg(Tagln-Cre)*			
Genotype	$Unc5b^{-/flox}$;+/*Tg(Tagln-Cre)*	$Unc5b^{+/flox}$;+/*Tg(Tagln-Cre)*	$Unc5b^{-/flox}$	$Unc5b^{+/flox}$
Number of progeny	18	10	7	11
Cross	$Unc5b^{flox/flox}$×$Unc5b^{+/-}$;+/*Tg(Nes-Cre)*			
Genotype	$Unc5b^{-/flox}$;+/*Tg(Nes-Cre)*	$Unc5b^{+/flox}$;+/*Tg(Nes-Cre)*	$Unc5b^{-/flox}$	$Unc5b^{+/flox}$
Number of progeny	6	12	6	9
Cross	$Unc5b^{flox/flox}$×$Unc5b^{+/-}$;+/*Tg(Wnt1-Cre)*			
Genotype	$Unc5b^{-/flox}$;+/*Tg(Wnt1-Cre)*	$Unc5b^{+/flox}$;+/*Tg(Wnt1-Cre)*	$Unc5b^{-/flox}$	$Unc5b^{+/flox}$
Number of progeny	4	8	6	3
Cross	$Unc5b^{flox/flox}$×$Unc5b^{+/-}$;+/*Tg(Vav-Cre)*			
Genotype	$Unc5b^{-/flox}$;+/*Tg(Vav-Cre)*	$Unc5b^{+/flox}$;+/*Tg(Vav-Cre)*	$Unc5b^{-/flox}$	$Unc5b^{+/flox}$
Number of progeny	17	23	14	8

Matings were performed between the genotypes indicated. Progeny were left with their mothers until weaning (3–4 weeks), at which time they were genotyped as described in the Materials and methods.

Table 2

Phenotypes of Unc5b deletion

A Diastolic flow reversal in umbilical arteries*

	Unc5b$^{+/flox}$; +/Tg(Tie2-Cre)			Unc5b$^{-/flox}$; +/Tg(Tie2-Cre)		
	Normal	**Reversed**	**Dead**	**Normal**	**Reversed**	**Dead**
Age (d.p.c.)	**Number of embryos**					
12	11	0	1	7	3	3
12.5	11	0	1	2	6	5
13	11	0	1	1	1	11
13.5	11	0	1	0	0	13

B Failure of rescue: *Unc5b*$^{+/-}$ × *Unc5b*$^{+/-}$ (morulae) + *Unc5b*$^{+/+}$ tetraploid (two cell)†

	Unc5b$^{+/+}$		*Unc5b*$^{+/-}$		*Unc5b*$^{-/-}$	
	Dead	Alive	Dead	Alive	Dead	Alive
Age (d.p.c.)	Number of embryos					
13.5	0	20	0	18	11	1

*Three pregnancies from *Unc5b*$^{flox/flox}$ × *Unc5b*$^{+/-}$; *Tg(Tie2-Cre)/Tg(Tie2-Cre)* crosses were probed at 12-hour intervals from E11.0 to E13.5. Umbilical flow and viability were monitored as described in the Materials and methods, and in the legend to Fig. 2. At E13.5, the pregnant females were sacrificed and the embryos genotyped.

†Morulae produced from an *Unc5b*$^{+/-}$ intercross were aggregated with tetraploid, wild-type, two-cell stage embryos. The fused embryos were implanted into females and allowed to mature. At E13.5 (relative age of the morulae), embryos were harvested, examined for viability and genotyped.